

# NUCLEOSYNTHESIS: WHAT DIRECT REACTIONS CAN DO FOR IT?\*

CARLOS A. BERTULANI

Department of Physics and Astronomy, Texas A&M University-Commerce  
Commerce, TX 75429, USA  
`carlos.bertulani@tamuc.edu`

(Received January 4, 2013)

The reactions of relevance for stellar evolution are difficult to measure directly in the laboratory at the small astrophysical energies. In recent years, indirect reaction methods have been developed and applied to extract low-energy astrophysical  $S$ -factors. These methods require a combination of new experimental techniques and theoretical efforts, which are the subject of this review.

DOI:10.5506/APhysPolB.44.531

PACS numbers: 24.10.-i, 26.50.+x, 25.60.-t

## 1. Introduction

**Fusion** — Fusion cross sections can be calculated from the equation [1]

$$\sigma_F(E) = \pi \lambda^2 \sum_{\ell} (2\ell + 1) P_{\ell}(E), \quad (1)$$

where  $E$  is the center of mass energy,  $\lambda = \sqrt{\hbar^2/2mE}$  is the reduced wavelength and  $\ell = 0, 1, 2, \dots$ . The cross section is proportional to  $\pi \lambda^2$ , the area of the quantum wave. Each part of the wave corresponds to different impact parameters having different probabilities for fusion. As the impact parameter increases, so does the angular momentum, hence the reason for the  $2\ell + 1$  term.  $P_{\ell}(E)$  is the probability that fusion occurs at a given impact parameter, or angular momentum. Sometimes, for a better visualization, or for extrapolation to low energies, one uses the concept of *astrophysical  $S$ -factor*, redefining the cross section as

$$\sigma_F(E) = \frac{1}{E} S(E) \exp[-2\pi\eta(E)], \quad (2)$$

---

\* Presented at the Zakopane Conference on Nuclear Physics “Extremes of the Nuclear Landscape”, Zakopane, Poland, August 27–September 2, 2012.

where  $\eta(E) = Z_1 Z_2 e^2 / \hbar v$ , with  $v$  being the relative velocity. The exponential function is an approximation to  $P_0(E)$  for a square-well nuclear potential plus Coulomb potential, whereas the factor  $1/E$  is proportional to the area appearing in Eq. (1).

**Many reaction channels** — Eq. (1) does not work in most situations. Only by including coupling to other channels, the fusion cross sections can be reproduced. In coupled channels schemes, one expands the total wavefunction for the system as

$$\Psi = \sum_i a_i(\alpha) \phi_i(\alpha, q_k), \quad (3)$$

where  $\phi$  form the channel basis,  $\alpha$  is a dynamical variable (*e.g.*, the distance between the nuclei), and  $q_k$  are intrinsic coordinates. Inserting this expansion in the Schrödinger equation yields a set of CC equations in the form [2]

$$\frac{da_k}{d\alpha} = \sum_j a_j \langle \phi_k | U | \phi_j \rangle e^{iE_\alpha \alpha / \hbar}, \quad (4)$$

where  $U$  is whatever potential couples the channels  $k$  and  $j$  and  $E_\alpha = E_\alpha^{(k)} - E_\alpha^{(j)}$  is some sort of transition energy, or transition momentum. In the presence of continuum states, continuum–continuum coupling (relevant for breakup channels) can be included by discretizing the continuum. This goes by the name of *Continuum Discretized Coupled-Channels* (CDCC) calculations. There are several variations of CC equations, *e.g.*, a set of differential equations for the wavefunctions, instead of using basis amplitudes. Coupled channels calculations with a large number of channels in continuum couplings are somewhat challenging: the phases of matrix elements can add destructively or constructively, depending on the system and on the nuclear model. Such suppressions or enhancements are difficult to interpret.

**Radiative capture** — For reactions involving light nuclei, only a few channels are of relevance. In this case, a real potential is enough for the treatment of fusion. For example, radiative capture cross sections of the type  $n + x \rightarrow a + \gamma$  and  $\pi L$  ( $\pi = E, (M) =$  electric (magnetic) L-pole) transitions can be calculated from [3]

$$\sigma_{EL, J_b}^{\text{d.c.}} = \text{const.} \times |\langle l_c j_c \| \mathcal{O}_{\pi L} \| l_b j_b \rangle|^2, \quad (5)$$

where  $\mathcal{O}_{\pi L}$  is an EM operator, and  $\langle l_c j_c \| \mathcal{O}_{\pi L} \| l_b j_b \rangle$  is a multipole matrix element involving bound ( $b$ ) and continuum ( $c$ ) wavefunctions. For electric multipole transitions ( $\mathcal{O}_{\pi L} = r^L Y_{LM}$ ),

$$\langle l_c j_c \| \mathcal{O}_{EL} \| l_b j_b \rangle = \text{const.} \times \int_0^\infty dr \, r^L u_b(r) u_c(r), \quad (6)$$

where  $u_i$  are radial wavefunctions. The total direct capture cross section is obtained by adding all multipolarities and final spins of the bound state ( $E \equiv E_{nx}$ ),

$$\sigma^{\text{d.c.}}(E) = \sum_{L, J_b} (\text{SF})_{J_b} \sigma_{L, J_b}^{\text{d.c.}}(E), \quad (7)$$

where  $(\text{SF})_{J_b}$  are spectroscopic factors.

**Asymptotic normalization coefficients** — In a microscopic approach, instead of single-particle wavefunctions one often makes use of overlap integrals,  $I_b(r)$ , and a many-body wavefunction for the relative motion,  $u_c(r)$ . Both  $I_b(r)$  and  $u_c(r)$  might be very complicated to calculate, depending on how elaborated the microscopic model is. The variable  $r$  is the relative coordinate between the nucleon and the nucleus  $x$ , with all the intrinsic coordinates of the nucleons in  $x$  being integrated out. The direct capture cross sections are obtained from the calculation of  $\sigma_{L, J_b}^{\text{d.c.}} \propto |\langle I_b(r) || r^L Y_L || \Psi_c(r) \rangle|^2$ .

The imprints of many-body effects will eventually disappear at large distances between the nucleon and the nucleus. One thus expects that the overlap function asymptotically matches ( $r \rightarrow \infty$ ),

$$I_b(r) = C_i \times \left( \frac{W_{-\eta, l_b+1/2}(2\kappa r)}{r} \right) \left[ \sqrt{\frac{2\kappa}{r}} K_{l_b+1/2}(\kappa r) \right], \quad (8)$$

where  $()$  are for protons and  $||$  for neutrons. The binding energy of the  $n + x$  system is related to  $\kappa$  by means of  $E_b = \hbar^2 \kappa^2 / 2m_{nx}$ ,  $W_{p,q}$  is the Whittaker function and  $K_\mu$  is the modified Bessel function. In Eq. (8),  $C_i$  is the *Asymptotic Normalization Coefficient* (ANC).

In the calculation of  $\sigma_{L, J_b}^{\text{d.c.}}$  above, one often meets the situation in which only the asymptotic part of  $I_b(r)$  and  $\Psi_c(r)$  contributes significantly to the integral over  $r$ . In these situations,  $u_c(r)$  is also well described by a simple two-body scattering wave (*e.g.* Coulomb waves). Therefore, the radial integration in  $\sigma_{L, J_b}^{\text{d.c.}}$  can be done accurately and the only remaining information from the many-body physics at short-distances is contained in the asymptotic normalization coefficient  $C_i$ , *i.e.*  $\sigma_{L, J_b}^{\text{d.c.}} \propto C_i^2$ . We thus run into an *effective theory for radiative capture cross sections*, in which the constants  $C_i$  carry all the information about the short-distance physics, where the many-body aspects are relevant [4]. It is worthwhile to mention that these arguments are reasonable for proton capture at very low energies, because of the Coulomb barrier.

**Resonating group method** — One immediate goal can be achieved in the coming years by using the *Resonating Group Method* (RGM) or the Generator Coordinate Method (GCM). These are a set of coupled integro-

differential equations of the form [5]

$$\sum_{\alpha'} \int d^3 r' [H_{\alpha\alpha'}^{AB}(\mathbf{r}, \mathbf{r}') - EN_{\alpha\alpha'}^{AB}(\mathbf{r}, \mathbf{r}')] g_{\alpha'}(\mathbf{r}') = 0, \quad (9)$$

where  $H(N)(\mathbf{r}, \mathbf{r}') = \langle \Psi_A(\alpha, \mathbf{r}) | H(1) | \Psi_B(\alpha', \mathbf{r}') \rangle$ . In these equations,  $H$  is the Hamiltonian for the system of two nuclei ( $A$  and  $B$ ) with the energy  $E$ ,  $\Psi_{A,B}$  is the wavefunction of nucleus  $A$  (and  $B$ ), and  $g_{\alpha}(\mathbf{r})$  is a function to be found by numerical solution of Eq. (9), which describes the relative motion of  $A$  and  $B$  in channel  $\alpha$ . Full antisymmetrization between nucleons of  $A$  and  $B$  are implicit. Modern nuclear shell-model calculations are able to provide the wavefunctions  $\Psi_{A,B}$  for light nuclei [6].

The astrophysical  $S$ -factor for the reaction  ${}^7\text{Be}(p, \gamma){}^8\text{B}$  was calculated [7] and excellent agreement was found with the experimental data in both direct and indirect measurements [7, 8]. The low- and high-energy slopes of the  $S$ -factor obtained with a many-body microscopic calculation [7] is well described by the fit

$$S_{17}(E) = (22.109 \text{ eV b}) \frac{1 + 5.30E + 1.65E^2 + 0.857E^3}{1 + E/0.1375}, \quad (10)$$

where  $E$  is the relative energy (in MeV) of  $p+{}^7\text{Be}$  in their center-of-mass. This equation corresponds to a Padé approximant of the  $S$ -factor. A sub-threshold pole due to the binding energy of  ${}^8\text{B}$  is responsible for the denominator [9, 10]. Figure 1 shows the world data on  ${}^7\text{Be}(p, \gamma){}^8\text{B}$  compared to a few of the theoretical calculations. The recent compilation published in Ref. [11] recommends  $S_{17} = 20.8 \pm 0.7$  (expt)  $\pm 1.4$  (theor) eV b.

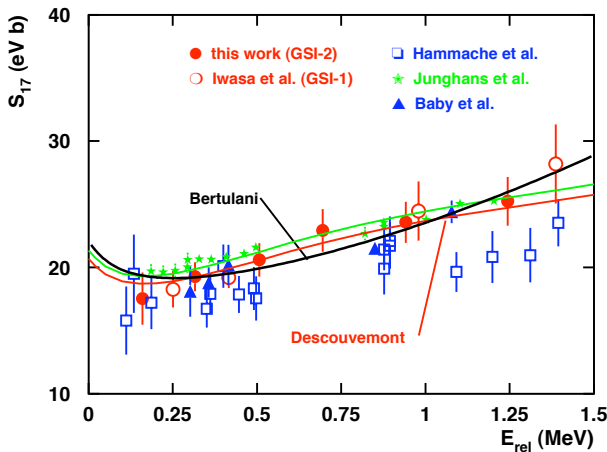


Fig. 1. World data on  ${}^7\text{Be}(p, \gamma){}^8\text{B}$  compared to theoretical calculations.

## 2. Direct reactions and the role of radioactive beams

**Transfer reactions** — Transfer reactions  $A(a, b)B$  are effective when a momentum matching exists between the transferred particle and the internal particles in the nucleus. Thus, beam energies should be in the range of a few 10 MeV per nucleon. Low energy reactions of astrophysical interest can be extracted directly from breakup reactions  $A+a \rightarrow b+c+B$  by means of the *Trojan Horse Method* (THM) [12]. If the Fermi momentum of the particle  $x$  inside  $a = (b+x)$  compensates for the initial projectile velocity  $v_a$ , the low energy reaction  $A+x = B+c$  is induced at very low (even vanishing) relative energy between  $A$  and  $x$ . Basically, this technique extends the method of transfer reactions to continuum states. Very successful results using this technique have been reported [13, 14].

Another transfer method, coined as ANC technique [4, 15, 16] relies on fact that the amplitude for the radiative capture cross section  $b+x \rightarrow a+\gamma$  is given by

$$M = \left\langle I_{bx}^a(\mathbf{r}_{bx}) | \mathcal{O}(\mathbf{r}_{bx}) | \psi_i^{(+)}(\mathbf{r}_{bx}) \right\rangle,$$

where

$$I_{bx}^a = \langle \phi_a(\xi_b, \xi_x, \mathbf{r}_{bx}) | \phi_x(\xi_x) \phi_b(\xi_b) \rangle$$

is the integration over the internal coordinates  $\xi_b$ , and  $\xi_x$ , of  $b$  and  $x$ , respectively. For low energies, the overlap integral  $I_{bx}^a$  is dominated by contributions from large  $r_{bx}$ . Thus, what matters for the calculation of the matrix element  $M$  is the asymptotic value of  $I_{bx}^a \sim C_{bx}^a W_{-\eta_a, 1/2}(2\kappa_{bx}r_{bx})/r_{bx}$ , where  $C_{bx}^a$  is the ANC and  $W$  is the Whittaker function. This coefficient is the product of the *spectroscopic factor* and a normalization constant which depends on the details of the wave function in the interior part of the potential. Thus,  $C_{bx}^a$  is the only unknown factor needed to calculate the direct capture cross section. These normalization coefficients can be found from: (1) analysis of classical nuclear reactions such as elastic scattering (by extrapolation of the experimental scattering phase shifts to the bound state pole in the energy plane), or (2) peripheral transfer reactions whose amplitudes contain the same overlap function as the amplitude of the corresponding astrophysical radiative capture cross section. One of the many advantages of using transfer reaction techniques over direct measurements is to avoid the treatment of the *electron screening problem* [13, 16].

**Intermediate energy Coulomb excitation** — The Coulomb excitation cross section is given by

$$\frac{d\sigma_{i \rightarrow f}}{d\Omega} = \left( \frac{d\sigma}{d\Omega} \right)_{\text{el}} \frac{16\pi^2 Z_2^2 e^2}{\hbar^2} \sum_{\pi\lambda\mu} \frac{B(\pi\lambda, I_i \rightarrow I_f)}{(2\lambda+1)^3} |S(\pi\lambda, \mu)|^2, \quad (11)$$

where  $B(\pi\lambda, I_i \rightarrow I_f)$  is the reduced transition probability of the projectile nucleus,  $\pi\lambda = E1, E2, M1, \dots$  is the multipolarity of the excitation, and  $\mu = -\lambda, -\lambda + 1, \dots, \lambda$ .

The relativistic corrections to the Rutherford formula for  $(d\sigma/d\Omega)_{\text{el}}$  (relevant for collisions at 50 MeV/nucleon and above) has been investigated in Ref. [17]. It was shown that the scattering angle increases by up to 6% when relativistic corrections are included in nuclear collisions at 100 MeV/nucleon. The effect on the elastic scattering cross section is even more drastic: up to 13% for center-of-mass scattering angles around 0–4 degrees.

The orbital integrals  $S(\pi\lambda, \mu)$  contain the information about relativistic corrections. Inclusion of absorption effects in  $S(\pi\lambda, \mu)$  due to the imaginary part of an optical nucleus–nucleus potential were worked out in Ref. [18]. These orbital integrals depend on the Lorentz factor  $\gamma = (1 - v^2/c^2)^{-1/2}$ , with  $c$  being the speed of light, on the multipolarity  $\pi\lambda\mu$ , and on the *adiabaticity parameter*  $\xi(b) = \omega_{\text{fi}} b / \gamma v < 1$ , where  $\omega_{\text{fi}} = (E_f - E_i) / \hbar$  is the excitation energy (in units of  $\hbar$ ) and  $b$  is the impact parameter.

Reference [19] has shown that at 10 MeV/nucleon the relativistic corrections are important only at the level of 1%. At 500 MeV/nucleon, the correct treatment of the recoil corrections is relevant on the level of 1%. Thus the non-relativistic treatment of Coulomb excitation [20] can be safely used for energies below about 10 MeV/nucleon and the relativistic treatment with a straight-line trajectory [21] is adequate above about 500 MeV/nucleon. However, at energies around 50 to 100 MeV/nucleon, accelerator energies common to most radioactive beam facilities, it is very important to use a correct treatment of *recoil and relativistic effects*, both kinematically and dynamically. At these energies, the corrections can add up to 50%. These effects were also shown in Ref. [22] for the case of excitation of giant resonances in collisions at intermediate energies.

A reliable extraction of useful nuclear properties, like the electromagnetic response ( $B(E2)$ -values,  $\gamma$ -ray angular distribution, *etc.*) from Coulomb excitation experiments at intermediate energies requires a proper treatment of special relativity [19, 23]. The dynamical relativistic effects have often been neglected in the analysis of experiments elsewhere (see, *e.g.* [24]). The effect is highly non-linear, *i.e.* a 10% increase in the velocity might lead to a 50% increase (or decrease) of certain physical observables. A general review of the importance of the relativistic dynamical effects in intermediate energy collisions has been presented in Ref. [2, 25].

**The Coulomb dissociation method** — The Coulomb dissociation method is quite simple. The (differential, or angle integrated) Coulomb breakup cross section for  $a + A \rightarrow b + c + A$  follows from Eq. (11). It can be rewritten as

$$\frac{d\sigma_{\text{C}}^{\pi\lambda}(\omega)}{d\Omega} = N^{\pi\lambda}(\omega; \theta; \phi) \cdot \sigma_{\gamma+a \rightarrow b+c}^{\pi\lambda}(\omega), \quad (12)$$

where  $\omega$  is the energy transferred from the relative motion to the breakup, and  $\sigma_{\gamma+a \rightarrow b+c}^{\pi\lambda}(\omega)$  is the photo nuclear cross section for the multipolarity  $\pi\lambda$  and photon energy  $\omega$ . The function  $N^{\pi\lambda}$ , sometimes called *virtual photon numbers*, depends on  $\omega$ , the relative motion energy, nuclear charges and radii, and the scattering angle  $\Omega = (\theta, \phi)$ .  $N^{\pi\lambda}$  can be reliably calculated [26] for each multipolarity  $\pi\lambda$ . Time reversal allows one to deduce the radiative capture cross section  $b+c \rightarrow a+\gamma$  from  $\sigma_{\gamma+a \rightarrow b+c}^{\pi\lambda}(\omega)$ . This method was proposed in Ref. [27] and has been tested successfully in a number of reactions of interest for astrophysics. The most celebrated case is the reaction  ${}^7\text{Be}(p, \gamma){}^8\text{B}$  [28], followed by numerous experiments in the last decade (see *e.g.* Ref. [29]).

Equation (12) is based on first-order perturbation theory. It also assumes that the nuclear contribution to the breakup is small, or that it can be separated under certain experimental conditions. The contribution of the nuclear breakup has been examined by several authors (see, *e.g.* [30]).  ${}^8\text{B}$  has a small proton separation energy ( $\approx 140$  keV). For such loosely-bound systems it had been shown that multiple-step, or higher-order effects, are important [31]. These effects occur by means of continuum–continuum transitions. Detailed studies of dynamic contributions to the breakup were explored in Refs. [32, 33] and in several other publications which followed. The role of higher multiplicities (*e.g.*,  $E2$  contributions [3, 34, 35] in the reaction  ${}^7\text{Be}(p, \gamma){}^8\text{B}$ ) and the coupling to high-lying states has also to be investigated carefully. Moreover, it has been shown that the influence of giant resonance states is small [36].

**Knock-out reactions** — The early interest in knockout reactions came from studies of nuclear halo states, for which the narrow momentum distributions of the core fragments in a qualitative way revealed the large spatial extension of the halo wave function. It was shown [37] that the longitudinal component of the momentum (taken along the beam or  $z$  direction) gave the most accurate information on the intrinsic properties of the halo and that it was insensitive to details of the collision and the size of the target. In contrast to this, the transverse distributions of the core are significantly broadened by diffractive effects and by Coulomb scattering. For experiments that observe the nucleon produced in elastic breakup, the transverse momentum is entirely dominated by diffractive effects, as illustrated [38] by the angular distribution of the neutrons from the reaction  ${}^9\text{Be}({}^{11}\text{Be}, {}^{10}\text{Be}+n)\text{X}$ . In this case, the width of the transverse *momentum distribution* reflects essentially the size of the target [39].

To test the influence of the medium effects in nucleon knockout reactions, we consider the removal of the  $l = 0$  halo neutron of  $^{15}\text{C}$ , bound by 1.218 MeV. The reaction studied is  ${}^9\text{Be}({}^{15}\text{C}, {}^{14}\text{C}_{\text{gs}})$ . The total cross sections as a function of the bombarding energy are shown in Fig. 2. The solid curve is obtained with the use of free nucleon–nucleon cross sections. The dashed curve includes the geometrical effects of Pauli blocking. The dashed-dotted curve is the result using the *Brueckner theory*, and the dotted curve is the phenomenological parametrization of the free cross section.

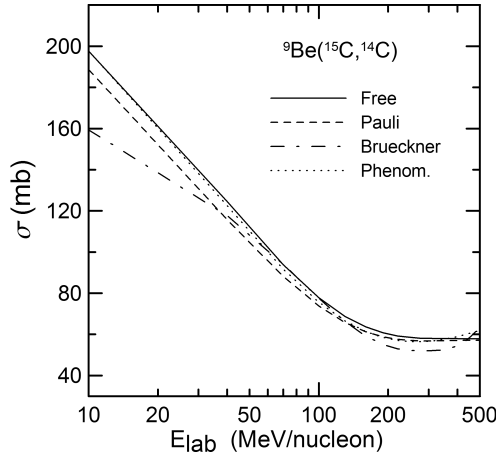


Fig. 2. Total knockout cross sections for removing the  $l = 0$  halo neutron of  $^{15}\text{C}$ , bound by 1.218 MeV, in the reaction  ${}^9\text{Be}({}^{15}\text{C}, {}^{14}\text{C}_{\text{gs}})$ . The solid curve is obtained with the use of free nucleon–nucleon cross sections. The dashed curve includes the geometrical effects of Pauli blocking. The dashed-dotted curve is the result using the *Brueckner theory*, and the dotted curve is a phenomenological parametrization.

In Fig. 3 we plot the longitudinal momentum distributions for the reaction  ${}^9\text{Be}({}^{11}\text{Be}, {}^{10}\text{Be})$ , at 250 MeV/nucleon [40]. The dashed curve is the cross section calculated using the  $NN$  cross section from the *Brueckner theory* and the solid curve is obtained the free cross section. One sees that the momentum distributions are reduced by 10%, about the same as the total cross sections, but the shape remains basically unaltered. If one rescales the dashed curve to match the solid one, the differences in the width are not visible [41].



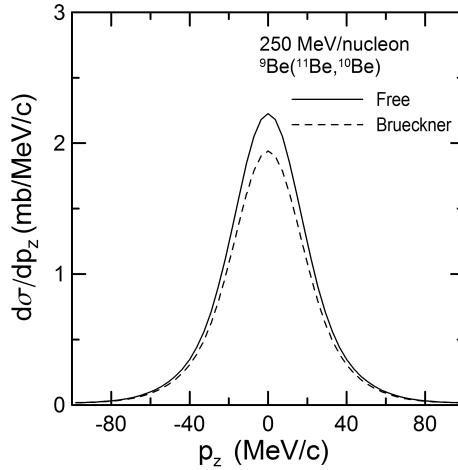


Fig. 3. Longitudinal momentum distribution for the residue in the  ${}^9\text{Be}({}^{11}\text{Be}, {}^{10}\text{Be})$ , reaction at 250 MeV/nucleon. The dashed curve is the cross section calculated using the  $NN$  cross section from the Brueckner theory and the solid curve is obtained the free cross section.

### 3. Conclusions

There were many questions not addressed in this review, such as the role of central nucleus–nucleus collisions in determining phase transition, equation of state, and a quark-gluon plasma, all topics of relevance in astrophysics. The review was more focused on the role of short-lived, exotic nuclei. There are many important scientific questions to be addressed both experimentally and theoretically in nuclear physics of exotic nuclei with relevance for astrophysics. These questions provide extreme challenges for experiments and theory. On the experimental side, producing the beams of radioactive nuclei needed to address the scientific questions has been an enormous challenge. Pioneering experiments have established the techniques and present-generation facilities have produced first exciting science results, but the field is still at the beginning of an era of discovery and exploration that will be fully underway once the range of next-generation facilities becomes operational. The theoretical challenges relate to wide variations in nuclear composition and rearrangements of the bound and continuum structure, sometimes involving near-degeneracy of the bound and continuum states. The extraction of reliable information from experiments requires a solid understanding of the reaction process, in addition to the structure of the nucleus. In astrophysics, new observations, for example the expected onset of data on stellar abundances, will require rare-isotope science for their interpretation.

The author acknowledge financial support from the U.S. Department of Energy Grants DE-FG02-08ER41533, DE-SC0004971.

## REFERENCES

- [1] L.F. Canto, P.R.S. Gomes, R. Donangelo, M.S. Hussein, *Phys. Rep.* **424**, 1 (2006).
- [2] C.A. Bertulani, *Phys. Rev. Lett.* **94**, 072701 (2005).
- [3] C.A. Bertulani, *Phys. Rev.* **C49**, 2688 (1994); *Nucl. Phys.* **A587**, 318 (1995); *Z. Phys.* **A356**, 293 (1996).
- [4] A.M. Mukhamedzhanov, N.K. Timofeyuk, *JETP Lett.* **51**, 282 (1990).
- [5] Y.C. Tang, M. LeMere, D.R. Thompson, *Phys. Rep.* **47**, 167 (1978).
- [6] S. Quaglioni, P. Navrátil, *Phys. Rev. Lett.* **101**, 092501 (2008).
- [7] P. Navrátil, C.A. Bertulani, E. Caurier, *Phys. Lett.* **B634**, 191 (2006); *Phys. Rev.* **C73**, 065801 (2006).
- [8] P. Navrátil, R. Roth, S. Quaglioni, [arXiv:1105.5977](https://arxiv.org/abs/1105.5977) [nucl-th].
- [9] B.K. Jennings, S. Karataglidis, T.D. Shoppa, *Phys. Rev.* **C58**, 579 (1998).
- [10] R.D. Williams, S.E. Koonin, *Phys. Rev.* **C23**, 2773 (1981).
- [11] E.G. Adelberger *et al.*, *Rev. Mod. Phys.* **83**, 195 (2011).
- [12] G. Baur, *Phys. Lett.* **B178**, 135 (1986).
- [13] M. La Cognata *et al.*, *Phys. Rev.* **C76**, 065804 (2007).
- [14] R.G. Pizzone *et al.*, *Few-Body Systems* **50**, 319 (2011).
- [15] R.E. Tribble *et al.*, *PoS*, online at: <http://pos.sissa.it/index.html>, 2007.
- [16] A.M. Mukhamedzhanov *et al.*, *J. Phys. Conf. Ser.* **202**, 012017 (2010).
- [17] C.E. Aguiar, A.N.F. Aleixo, C.A. Bertulani, *Phys. Rev.* **C42**, 2180 (1990).
- [18] C.A. Bertulani, A.M. Nathan, *Nucl. Phys.* **A554**, 158 (1993).
- [19] C.A. Bertulani, A. Stuchbery, T. Mertzimekis, A. Davies, *Phys. Rev.* **C68**, 044609 (2003).
- [20] K. Alder, A. Winther, *Electromagnetic Excitation*, North-Holland, Amsterdam 1975.
- [21] A. Winther, K. Alder, *Nucl. Phys.* **A319**, 518 (1979).
- [22] A.N.F. Aleixo, C.A. Bertulani, *Nucl. Phys.* **A505**, 448 (1989).
- [23] C.A. Bertulani, C.M. Campbell, T. Glasmacher, *Comput. Phys. Commun.* **152**, 317 (2003).
- [24] T. Glasmacher, *Nucl. Phys.* **A693**, 90 (2001).
- [25] C.A. Bertulani, [arXiv:nuc1-th/0505015](https://arxiv.org/abs/nuc1-th/0505015).
- [26] C.A. Bertulani, G. Baur, *Phys. Rep.* **163**, 299 (1988).
- [27] G. Baur, C. Bertulani, H. Rebel, *Nucl. Phys.* **A458**, 188 (1986).

- [28] T. Motobayashi *et al.*, *Phys. Rev. Lett.* **73**, 2680 (1994).
- [29] H. Esbensen, G.F. Bertsch, K. Snover, *Phys. Rev. Lett.* **94**, 042502 (2005); M. Gai, *Phys. Rev. Lett.* **96**, 159201 (2006).
- [30] C.A. Bertulani, M. Gai, *Nucl. Phys.* **A636**, 227 (1998).
- [31] C.A. Bertulani, L.F. Canto, *Nucl. Phys.* **A539**, 163 (1992).
- [32] G. Baur, C.A. Bertulani, D.M. Kalassa, *Nucl. Phys.* **A550**, 527 (1992).
- [33] G.F. Bertsch, C.A. Bertulani, *Nucl. Phys.* **A556**, 136 (1993); *Phys. Rev.* **C49**, 2839 (1994); H. Esbensen, G.F. Bertsch, C.A. Bertulani, *Nucl. Phys.* **A581**, 107 (1995).
- [34] M. Gai, C.A. Bertulani, *Phys. Rev.* **C52**, 1706 (1995); *Nucl. Phys.* **A636**, 227 (1998).
- [35] H. Esbensen G. Bertsch, *Phys. Lett.* **B359**, 13 (1995); *Nucl. Phys.* **A600**, 37 (1996).
- [36] C.A. Bertulani, *Phys. Lett.* **B547**, 205 (2002).
- [37] C.A. Bertulani, K.W. McVoy, *Phys. Rev.* **C46**, 2638 (1992).
- [38] R. Anne *et al.*, *Nucl. Phys.* **A575**, 125 (1994).
- [39] C.A. Bertulani, P.G. Hansen, *Phys. Rev.* **C70**, 034609 (2004).
- [40] C.A. Bertulani, C. De Conti, *Phys. Rev.* **C81**, 064603 (2010).
- [41] M. Karakoc, A. Banu, C.A. Bertulani, L. Trache, *Phys. Rev.* **C** (2013), in press.